JOC*Article*

Kinetic Studies of a Fast, Reversible Alkene Radical Cation Cyclization Reaction

John H. Horner and Martin Newcomb*

Department of Chemistry, University of Illinois at Chicago, 845 West Taylor Street, Chicago, Illinois 60607

men@uic.edu

Received September 9, 2006

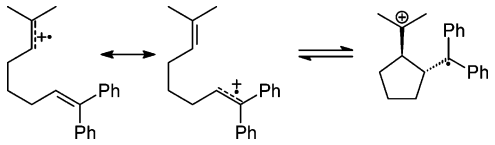

The radical cation formed by mesylate heterolysis from the 1,1-dimethyl-7,7-diphenyl-2-mesyloxy-6-heptenyl radical was studied in several solvents. Computational results suggest that the initially formed acyclic radical cation is a resonance hybrid with partial positive charge in both double bonds of 1,1-diphenyl-7-methyl-1,6-octadiene (**10**). Thiophenol trapping was used as the competing reaction for kinetic determinations. The acyclic radical cation rapidly equilibrates with a cyclic distonic radical cation, and thiophenol trapping gives acyclic product **10** and cyclic products, mainly *trans*-1-(diphenylmethyl)-2-(1-methylethenyl)cyclopentane (**11**). The rate constants for cyclization at ambient temperature were $k = (0.5-2) \times 10^{10}$ s^{-1}, and those for ring opening were $k = (1.5-9) \times 10^{10}$ s^{-1}. Laser flash photolysis studies in several solvents show relatively slow processes ($k = (2.5-260) \times 10^5$ s^{-1}) that involve rate-limiting trapping reactions for the equilibrating radical cations. In mixtures of fluoroalcohols R_fCH_2OH in trifluoromethylbenzene, variable-temperature studies display small, and in one case a negative, activation energies, requiring equilibration reactions prior to the rate-limiting processes. Fast equilibration of acyclic and cyclic radical cations implies that product ratios can be controlled by the populations of the acyclic and cyclic species and relative rate constants for trapping each.

Introduction

Radical cations are open-shell intermediates that offer unique reactivity patterns, more reactive than a radical but more controllable than a cation.[1,2] Typically, radical cations are formed from unsaturated compounds by chemical,[3] electrochemical,[4,5] or photochemical[6] one-electron oxidation reactions, but they also can be produced by heterolytic fragmentation of radicals containing β-leaving groups.[7−9] In synthetic applications, an attractive feature of radical cation formation by radical heterolysis reactions is that nucleophilic trapping can be faster than molecular correlation times, permitting diastereoselective reactions that preserve chirality in a putative achiral intermediate.[10,11]

Despite the potential utility of radical cations in synthesis, some reaction types are not well developed. For example, cationic and radical cyclization reactions that form five- or six-membered ring carbocycles are well-known, but related cyclization reactions involving a radical cation adding to an alkene are less well studied.[12] A radical cation cycloaddition reaction[13] can maintain conjugation that is present in the reactant, but a 5-*exo* or 6-*exo* cyclization reaction would convert a localized, conjugated radical cation into a distonic radical cation. Such a

(1) Schmittel, M.; Burghart, A. *Angew. Chem., Int. Ed.* **1997**, *36*, 2550−2589.
(2) Tanko, J. M.; Phillips, J. P. *J. Am. Chem. Soc.* **1999**, *121*, 6078−6079.
(3) Bauld, N. L. *Tetrahedron* **1989**, *45*, 5307−5363.
(4) Moeller, K. D. *Tetrahedron* **2000**, *56*, 9527−9554.
(5) Reddy, S. H. K.; Chiba, K.; Sun, Y. M.; Moeller, K. D. *Tetrahedron* **2001**, *57*, 5183−5197.
(6) Mangion, D.; Arnold, D. R. *Acc. Chem. Res.* **2002**, *35*, 297−304.
(7) Beckwith, A. L. J.; Crich, D.; Duggan, P. J.; Yao, Q. W. *Chem. Rev.* **1997**, *97*, 3273−3312.
(8) Crich, D. In *Radicals in Organic Synthesis*; Renaud, P., Sibi, M. P., Eds.; Wiley-VCH: Weinheim, 2001; Vol. 2, pp 188−206.
(9) Crich, D.; Brebion, F.; Suk, D.-H. *Top. Curr. Chem.* **2006**, *263*, 1−38.
(10) Crich, D.; Shirai, M.; Rumthao, S. *Org. Lett.* **2003**, *5*, 3767−3769.
(11) Crich, D.; Ranganathan, K. *J. Am. Chem. Soc.* **2005**, *127*, 9924−9929.
(12) See: Huang, Y. T.; Moeller, K. D. *Org. Lett.* **2004**, *6*, 4199−4202 and references therein.
(13) Bauld, N. L.; Bellville, D. J.; Harirchian, B.; Lorenz, K. T.; Pabon, R. A., Jr.; Reynolds, D. W.; Wirth, D. D.; Chiou, H. S.; Marsh, B. K. *Acc. Chem. Res.* **1987**, *20*, 371−378.

10.1021/jo061868w CCC: $37.00
Published on Web 01/27/2007

SCHEME 1

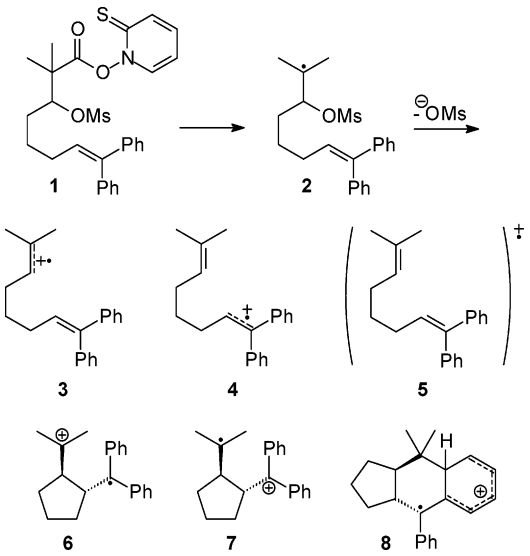

SCHEME 2

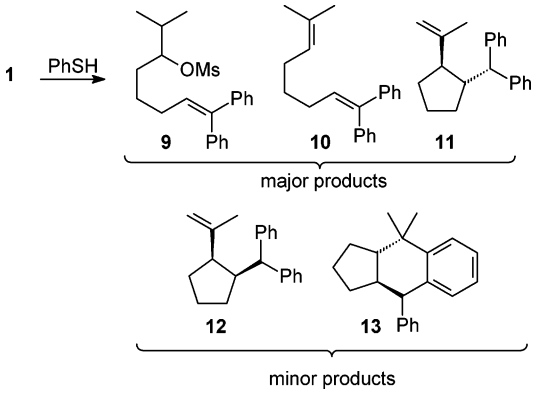

reaction might be thermodynamically disfavored unless the distonic radical cation contains good cation- and/or radical-stabilizing groups. Nonetheless, because localized and distonic radical cations can demonstrate much different reactivities in follow-up reactions including nucleophilic captures and secondary oxidations, carbocyclizations of alkene radical cations might be successful even if thermodynamically disfavored when the timings of the follow-up reactions are appropriate.

We have studied radical cation cyclization reactions to understand the kinetics of their reactions better and with the aim of developing radical cation probes[14] or clocks[15,16] that can be used in indirect kinetic studies.[17] We describe here kinetic studies of an alkene radical cation 5-*exo* cyclization reaction that provide rate and equilibrium constants for the cyclization and reverse reaction in a variety of solvents. As one would expect, the cyclization and ring-opening reactions of alkene radical cations are several orders of magnitude faster than the corresponding reactions of radicals.

Results

The system we studied is described in Scheme 1, which shows possible transients, and Scheme 2, which shows products. The PTOC ester[18,19] **1** was prepared from the corresponding carboxylic acid as described in the Supporting Information. Radical precursor **1** reacted in laser flash photolysis (LFP) reactions and in photoinitiated radical chain reactions to give the β-mesylate radical **2**. It is important to note that, although LFP and photoinitiation methods were employed, the reactions studied in this work are those of electronic ground-state species and *not* photochemical reactions. Heterolytic fragmentation of the mesylate group in **2** can give radical cation **3** as the initial product, which might react by internal electron transfer to give the isomeric radical cation **4**, but computational results suggest that the most stable "acyclic" radical cation is species **5**, which is a resonance hybrid of **3** and **4** (see below). Irrespective of the detailed structure of the acyclic radical cation, it can react in 5-*exo* cyclization reactions to give distonic radical cations **6** and **7**, and other cyclic transient radical cations, such as **8**, can be formed.

The products obtained from preparative scale radical chain reactions of precursor **1** in the presence of thiophenol are shown in Scheme 2. The major products formed were mesylate **9**, diene **10**, and *trans*-cyclization product **11**, and each of these was identified by comparison to an authentic sample that was prepared for characterization purposes. Several minor products were detected in the reaction mixtures, and samples of two of those, *cis*-cyclization product **12** and *trans*-tricyclic product **13**, also were independently prepared. The Friedel−Crafts cyclization product **13** was previously reported to be formed from reaction of diene **10**.[20]

Computational studies were used as a guide for understanding the species formed in the reactions we studied. Enthalpies of reactions forming radical cations **3**−**5** by oxidations of diene **10** were estimated by DFT calculations[21] (B3LYP/6-31G*) via the reactions outlined in Scheme 3. The enthalpy change for oxidation of diene **10** to the delocalized system **5** was computed from an isodesmic reaction of **10** with the ethylene radical cation. For the localized radical cations **3** and **4**, we estimated that the enthalpy changes upon oxidation would be approximately equal to those for oxidations of the alkenes **14** and **15** and computed the enthalpy change for the isodesmic reactions of these alkenes with the ethylene radical cation. From these results (see Supporting Information), the resonance hybrid

(14) Schepp, N. P.; Shukla, D.; Sarker, H.; Bauld, N. L.; Johnston, L. J. *J. Am. Chem. Soc.* **1997**, *119*, 10325−10334.

(15) Newcomb, M.; Miranda, N.; Sannigrahi, M.; Huang, X.; Crich, D. *J. Am. Chem. Soc.* **2001**, *123*, 6445−6446.

(16) Horner, J. H.; Taxil, E.; Newcomb, M. *J. Am. Chem. Soc.* **2002**, *124*, 5402−5410.

(17) Newcomb, M. *Tetrahedron* **1993**, *49*, 1151−1176.

(18) PTOC is an abbreviation for pyridine-2-thioneoxycarbonyl. PTOC esters react in chain reactions to give acyloxyl radicals that rapidly decarboxylate to give alkyl radicals. For details, see ref 19.

(19) Barton, D. H. R.; Crich, D.; Motherwell, W. B. *Tetrahedron* **1985**, *41*, 3901−3924.

(20) Ishii, H.; Yamaoka, R.; Imai, Y.; Hirano, T.; Maki, S.; Niwa, H.; Hashizume, D.; Iwasaki, F.; Ohashi, M. *Tetrahedron Lett.* **1998**, *39*, 9501−9504.

(21) Frisch, M. J.; Trucks, G. W.; Schlegel, H. B.; Scuseria, G. E.; Robb, M. A.; Cheeseman, J. R.; Zakrzewski, V. G.; Montgomery, J. A., Jr.; Stratmann, R. E.; Burant, J. C.; Dapprich, S.; Millam, J. M.; Daniels, A. D.; Kudin, K. N.; Strain, M. C.; Farkas, O.; Tomasi, J.; Barone, V.; Cossi, M.; Cammi, R.; Mennucci, B.; Pomelli, C.; Adamo, C.; Clifford, S.; Ochterski, J.; Petersson, G. A.; Ayala, P. Y.; Cui, Q.; Morokuma, K.; Malick, D. K.; Rabuck, A. D.; Raghavachari, K.; Foresman, J. B.; Cioslowski, J.; Ortiz, J. V.; Stefanov, B. B.; Liu, G.; Liashenko, A.; Piskorz, P.; Komaromi, I.; Gomperts, R.; Martin, R. L.; Fox, D. J.; Keith, T.; Al-Laham, M. A.; Peng, C. Y.; Nanayakkara, A.; Gonzalez, C.; Challacombe, M.; Gill, P. M. W.; Johnson, B. G.; Chen, W.; Wong, M. W.; Andres, J. L.; Head-Gordon, M.; Replogle, E. S.; Pople, J. A. *Gaussian 98*, revision A.9; Gaussian, Inc.: Pittsburgh, PA, 1998.

SCHEME 3

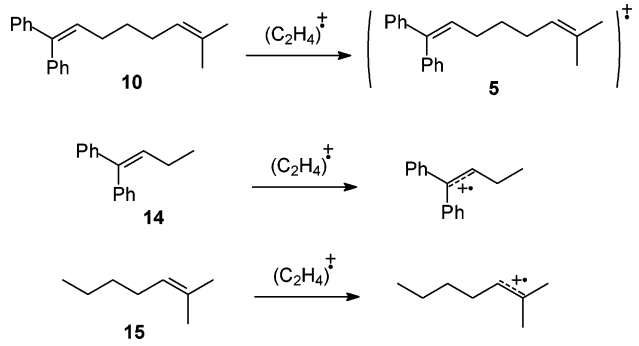

SCHEME 4

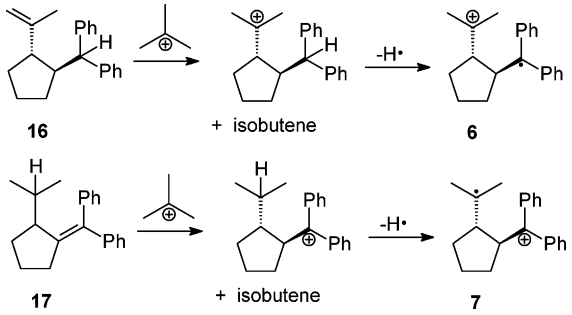

radical cation **5** was computed to be 4 kcal/mol more stable than radical cation **4** and 23 kcal/mol more stable than **3**.[22]

As a delocalized species, resonance hybrid **5** would be expected to be lower in energy than either of the localized radical cations, **3** and **4**. The computational results indicate that the positive charge in **5** is concentrated mainly (85%) on the diphenylethene moiety. Both double bonds in diene **10** are lengthened upon oxidation to **5**. The phenyl-substituted C1−C2 double bond in **5** is 4.0 pm longer than the corresponding double bond in diene **10**, whereas the C6−C7 double bond in **5** is only 1.7 pm longer than the C6−C7 double bond in **10**.

Computations of the enthalpies of formation of the cyclic distonic radical cations **6** and **7** were less straightforward than those above because the radical and cation centers are not in one moiety. We made the assumption that the distonic species behaved as if the cation and radical centers were isolated from each other and did not interact. In fact, these centers are close enough such that they might interact with one another, but a cancellation of errors was expected when the energetics of the two distonic radical cations were compared. We calculated the enthalpy of reactions for the closed shell compounds **16** and **17** reacting with the *tert*-butyl cation by hydride transfer to estimate the proton affinities of the cationic intermediates shown in Scheme 4. The bond dissociation energies (BDEs) of these species were then approximated using BDE values from the literature; specifically, we used C−H BDE values of 96 kcal/mol for isobutane and 80 kcal/mol for 1,1-diphenylethane for the estimates.[23−25]

The approach in Scheme 4 indicated that distonic radical cation **6** was approximately 6 kcal/mol more stable than distonic radical cation **7**. The gas-phase computational results cannot be trusted to provide highly accurate energies for charged species in solution, of course, but the prediction that **6** is more stable than **7** is supported by experimental studies of a related distonic radical cation species; radical cation **18** was favored over **19** in low-polarity media, whereas **18** and **19** were of comparable energies in a moderate-polarity solvent.[26] Interestingly, the absolute enthalpy for distonic radical cation **6** was only slightly greater (2 kcal/mol) than that of the delocalized acyclic radical cation **5**, and this enthalpy ranking and difference closely match the experimental results discussed below in that the equilibrium between cyclization and ring opening slightly favored the acyclic species.

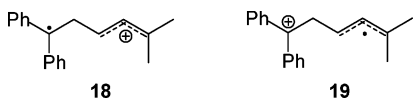

Thiophenol Trapping Studies. Heterolysis of the mesylate group in radical **2** was demonstrated in a series of trapping studies that have been reported.[27] In brief, radical **2** reacted rapidly by heterolysis to give an acyclic radical cation that was initially formed in a contact ion pair (CIP), and rate constants for the heterolysis reaction that produces the CIP, for collapse of the CIP back to neutral radical **2**, and for solvation of the CIP to give a solvent-separated ion pair (SSIP) or free ions were determined.[27] These processes are quite fast, and mesylate heterolysis to give radical cations occurred with half-lives of 1−20 ns at ambient temperature.[27]

In preparative reactions studied in this work, radical precursor **1** was allowed to react in chain reactions in the presence of thiophenol. Trapping studies were performed with varying concentrations of PhSH in several solvents and solvent mixtures at ambient temperature. PTOC ester **1** at ca. 10 mM concentration was allowed to react in radical chain reactions that were initiated by visible light photolysis. It is important to note that the reactions were for radicals and radical cations in the ground state; we did not study photochemical reactions. Following the reactions, products were identified by HPLC, NMR spectroscopy, and GC mass spectrometry. The major products were mesylate **9**, diene **10**, and *trans*-cyclization product **11**, and minor products also were obtained (Scheme 2). The yields of various products were determined by quantitative HPLC. GC could not be used for quantitative results because mesylate **9** decomposed thermally to give, in part, diene **10**. The mesylate product **9**, diene **10**, and cyclization product **11** accounted for more than 90% of the products. Figure 1 shows a typical HPLC result where minor products are apparent.

For representative results of the trapping studies, we listed in Table 1 the ratio of acyclic product **10** to the total amounts of cyclic products obtained when 1 M thiophenol was employed. Detailed results of the trapping studies are given in Tables S1−S6 in the Supporting Information, and Figure 2 shows plots of acyclic product **10** to cyclic product ratios for three sets of studies. In Figure 2, four analyses for one or two reactions per thiophenol concentration were used to give average results with

(22) We judge the results to be reliable at the semiquantitative level because similar computations for isodesmic reactions of alkenes with known ionization potentials with an ethylene radical cation had average errors of 2.2 kcal/mol; see Supporting Information.

(23) Rossi, M. J.; McMillen, D. F.; Golden, D. M. *J. Phys. Chem.* **1984**, *88*, 5031−5039.

(24) Berkowitz, J.; Ellison, G. B.; Gutman, D. *J. Phys. Chem.* **1994**, *98*, 2744−2765.

(25) Halgren, T. A.; Roberts, J. D.; Horner, J. H.; Martinez, F. N.; Tronche, C.; Newcomb, M. *J. Am. Chem. Soc.* **2000**, *122*, 2988−2994.

(26) Horner, J. H.; Bagnol, L.; Newcomb, M. *J. Am. Chem. Soc.* **2004**, *126*, 14979−14987.

(27) Horner, J. H.; Lal, M.; Newcomb, M. *Org. Lett.* **2006**, *8*, 5497−5500.

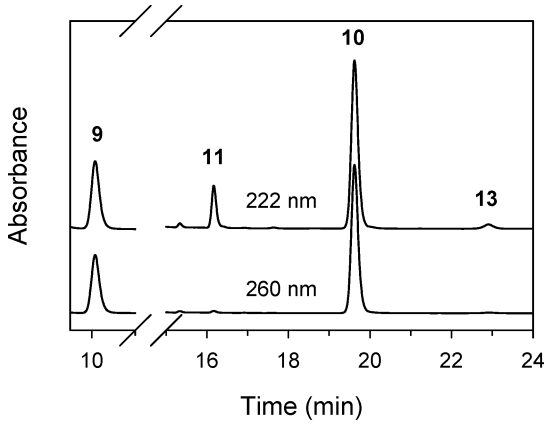

FIGURE 1. Portion of HPLC trace (reversed-phase C18 column, acetonitrile/methanol/water elution) from reaction of **1** in CH_2Cl_2 in the presence of 2.0 M PhSH monitored at 222 and 260 nm. Products **9**−**11** and **13** are labeled with their compound numbers. Product **12** coelutes with **11** under these conditions, but **12** was shown to be a minor component by GC mass spectrometry.

TABLE 1. Kinetics from Thiophenol Trapping Experiments[a]

solvent	$E_T(30)$[b]	[**10**]/[cyclics][c]	k_{cycle} (10^{10} s^{-1})	k_{open} (10^{10} s^{-1})
benzene	34.3	12 ± 3		
$PhCF_3$	38.5	6 ± 2	1.3 ± 0.2	7.0 ± 1.1
CH_2Cl_2	40.7	3.3 ± 0.1	1.8 ± 0.1	3.9 ± 0.3
CH_3CN	45.6	5.8 ± 0.3	1.8 ± 0.8	9 ± 4
0.5% TFE/TFT[d]	52.8	5 ± 1	0.87 ± 0.08	2.7 ± 0.4
1% TFE/TFT[d]	53.8	6.2 ± 0.6	0.56 ± 0.03	1.5 ± 0.2

[a] Rate constants at ambient temperature with errors at 2σ; detailed results are in the Supporting Information. [b] $E_T(30)$ solvent polarity value from ref 34 for pure solvents and measured for mixtures of TFE in TFT. [c] Average ratio of acyclic product **10** to cyclic products for reactions conducted in the presence of 1.0 M PhSH. [d] TFE = 2,2,2-trifluoroethanol; TFT = trifluorotoluene.

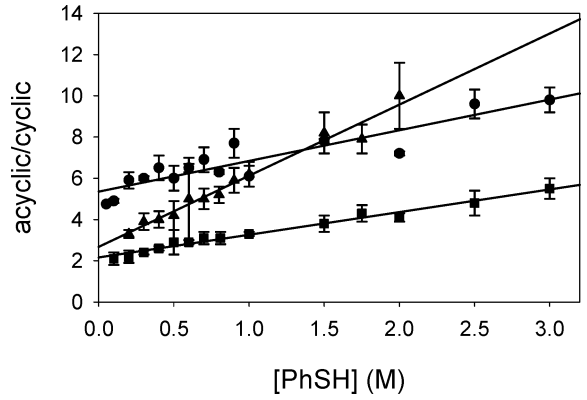

FIGURE 2. Ratios of acyclic product **10** to cyclic products from thiophenol trapping reactions in trifluorotoluene (●), methylene chloride (■), and trifluorotoluene containing 1% 2,2,2-trifluoroethanol (▲). The lines are fits from eq 1.

errors at 2σ that are shown on the plots. The plots of thiophenol trapping results demonstrate a competitive reaction sequence[17] in which an acyclic radical cation is in equilibrium with one or more transients that react to give cyclic products (Scheme 5). The shallow slopes in the product ratio plots show that thiophenol trapping of the acyclic radical cation(s) was competitive with the cyclization reactions, and the nonzero intercepts

SCHEME 5

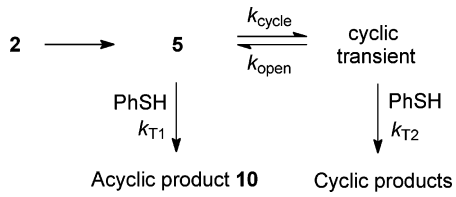

of the plots required that formation of the cyclic transient be reversible in the time frame of thiophenol trapping of the radical cations.[17]

The competition reaction sequence is shown in Scheme 5, and the ratio of acyclic product **10** to cyclic products is described by eq 1,[17] where the rate constants are those shown in Scheme 5. Solution of the experimental results by nonlinear regression analysis gives ratios of rate constants that contain k_{cycle} and k_{open}. These ratios will provide absolute rate constants for the cyclization and ring-opening reaction in Scheme 5 if the rate constants for the thiophenol reactions are known or estimated.

$$\textbf{[10]}/[\text{cyclic products}] = (k_{T1}k_{open})/(k_{T2}k_{cycle}) + (k_{T1}[\text{PhSH}])/k_{cycle} \quad (1)$$

We assume that the bimolecular trapping reaction of the acyclic radical cation by PhSH is a diffusion-controlled reaction based on the large difference in oxidation potentials for 2-methyl-2-butene[28] and thiophenol[29] of 1.2 V. Similar assumptions that PhSH trapping of radical cations would be a diffusion-controlled process were made previously by others.[26,30,31] The diffusional rate constant for thiophenol, k_{diff}, estimated from the von Smulochowski equation[32] and the Stokes−Einstein equation[33] is 2×10^{10} M^{-1} s^{-1} at ambient temperature. With this value for k_{T1} in Scheme 5, the first-order rate constants for cyclization of the radical cations can be calculated from the slopes of the plots in Figure 2.

The rate constants for the cyclization reaction are in good agreement with one another and vary little with solvent polarity as judged by the $E_T(30)$ solvent polarity values,[34] which are listed in Table 1. The cyclization reactions are very fast, with rate constants in the 10^{10} s^{-1} range. It is noteworthy that 5-*exo* cyclization reactions of radicals have log *A* terms in their Arrhenius functions in the range of 9.5−10.5.[17,35,36] If the log *A* values for cyclization of radical cation **5** are in a similar range, then the entropy-limited rate constants for cyclization at any temperature would be in the range of 3×10^9 to 3×10^{10} s^{-1}, which is comparable to the experimental values in Table 1. Thus, the cyclization reactions of the acyclic radical cation apparently have very small or zero activation energies such that they are highly or completely under entropic control.

(28) Schepp, N. P.; Johnston, L. J. *J. Am. Chem. Soc.* **1996**, *118*, 2872−2881.
(29) Armstrong, D. A.; Sun, Q.; Schuler, R. H. *J. Phys. Chem.* **1996**, *100*, 9892−9899.
(30) Giese, B.; Burger, J.; Kang, T. W.; Kesselheim, C.; Wittmer, T. *J. Am. Chem. Soc.* **1992**, *114*, 7322−7324.
(31) Giese, B.; Beyrich-Graf, X.; Burger, J.; Kesselheim, C.; Senn, M.; Schafer, T. *Angew. Chem., Int. Ed. Engl.* **1993**, *32*, 1742−1743.
(32) Schuh, H. H.; Fischer, H. *Helv. Chim. Acta* **1978**, *61*, 2130−2164.
(33) Edward, J. T. *J. Chem. Educ.* **1970**, *47*, 261−270.
(34) Reichardt, C. *Chem. Rev.* **1994**, *94*, 2319−2358.
(35) Newcomb, M.; Horner, J. H.; Filipkowski, M. A.; Ha, C.; Park, S. U. *J. Am. Chem. Soc.* **1995**, *117*, 3674−3684.
(36) Johnson, C. C.; Horner, J. H.; Tronche, C.; Newcomb, M. *J. Am. Chem. Soc.* **1995**, *117*, 1684−1687.

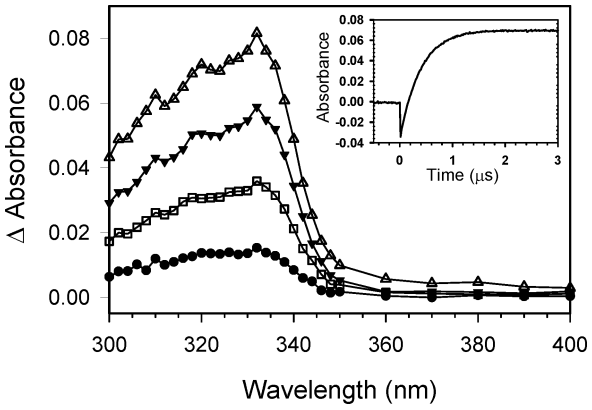

FIGURE 3. Time-resolved UV−visible spectrum from reaction of **1** in CH_2Cl_2 showing growth of diphenylalkyl radical signals with λ_{max} = 334 nm; no growth in absorbance was observed for longer wavelengths than shown here. The time slices are at 207 ns (●), 351 ns (□), 607 ns (▼), and 1.98 μs (△) after the laser pulse. Traces at the indicated times were obtained by subtracting the raw spectra from the spectrum at 130 ns. The inset shows the kinetic trace at 334 nm.

SCHEME 6

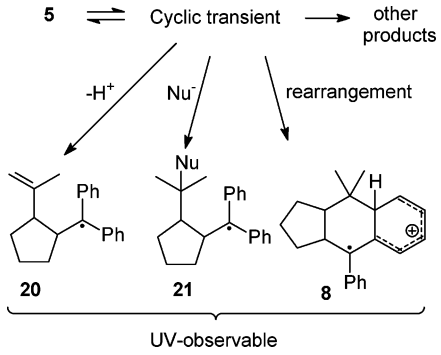

Because plots of acyclic product **10** to cyclic product have measurable intercepts (cf. Figure 2), it is possible to calculate a ratio that contains the ring-opening rate constant for the cyclic transient, k_{open}/k_{T2}.[17] If we assume that thiophenol reacts with the cyclic distonic radical cation in diffusion-controlled reactions, then $k_{T2} = 2 \times 10^{10}$ M^{-1} s^{-1} at ambient temperature, and we can calculate rate constants for k_{open}. Values thus calculated are listed in Table 1. The apparent result is that the ring-opening reaction is very fast, and the equilibrium between an acyclic radical cation and a cyclic distonic radical cation favors the acyclic species. The assumption that PhSH trapping of the cyclic distonic radical cations is a diffusion-controlled process is not as firm as the assumption that reduction of the acyclic radical cation will be diffusion controlled because the mode(s) of reaction of the distonic radical cations with PhSH are not known. Therefore, it is possible that the rate constant k_{T2} in Scheme 5 is smaller than the diffusion-control limit, and accordingly, the equilibrium in Scheme 5 will be more favorable for the cyclic product. Despite that caveat, the equilibrium constant values in Table 1 appear to be consistent with both LFP studies and computational results discussed above.

Whereas the cyclization reactions approach the entropic limit for a 5-*exo* cyclization with a small or zero activation energy, the ring-opening reactions have larger activation energies. The entropic demand for ring-opening reactions is small, with log *A* values on the order of 12 to 13. For a ring-opening reaction with a rate constant in the range of $(1-10) \times 10^{10}$ s^{-1} at ambient temperature as found here, the activation energy for the process is in the range of 2−4 kcal/mol.

TABLE 2. Rate Constants and Arrhenius Parameters from LFP Experiments[a]

solvent[b]	$E_T(30)$[c]	$k_{(20\,°C)}$ (s^{-1})	log *A*	E_a (kcal/mol)
$PhCF_3$ (TFT)	38.5	2.5 ± 10^5	10.1	6.3 ± 0.4
TFT/0.5% TFE	52.8	2.4 ± 10^6	8.4 ± 0.3	2.7 ± 0.4
TFT/0.0125 M F2	48.5	5.8 ± 10^5	8.3 ± 0.2	3.4 ± 0.2
TFT/0.025 M F2	49.8	1.0 ± 10^6	7.8 ± 0.1	2.4 ± 0.1
TFT/0.05 M F1	51.8	2.6 ± 10^6	7.9 ± 0.1	2.0 ± 0.1
TFT/0.1 M F1	52.5	7.5 ± 10^6	6.9 ± 0.1	0.03 ± 0.2
TFT/0.2 M F1	53.2	2.6 ± 10^7	6.3 ± 0.3	-1.5 ± 0.5
CH_2Cl_2	40.7	2.6 ± 10^6		
CH_3CN	45.6	4.7 ± 10^6	10.7 ± 0.2	5.4 ± 0.2
CH_3CN/5% TFE	55.6	6.0 ± 10^6	11.1 ± 0.3	5.8 ± 0.3

[a] Kinetic results for growth of a signal at 334 nm following irradiation of PTOC precursor **2** with 355 nm laser light. [b]TFT = trifluorotoluene; TFE = 2,2,2-trifluoroethanol; F1 = 2,2,3,3,4,4,5,5-octafluoropentanol; F2 = 2,2,3,3,4,4,5,5,6,6,7,7,8,8,8-pentadecafluorooctanol. [c]Measured $E_T(30)$ values; see ref 34.

Laser Flash Photolysis (LFP) Studies. We conducted LFP studies in methylene chloride, trifluorotoluene (TFT), and acetonitrile and in TFT and CH_3CN solutions containing 2,2,2-trifluoroethanol (TFE) or other fluorinated alcohols to increase solvent polarity. In these studies, PTOC ester **1** again was the radical precursor. Irradiation of **1** with 355 nm laser light (third harmonic of a Nd:YAG laser) gave an acyloxyl radical and the pyridine-2-thiyl radical as first-formed intermediates. Subnanosecond decarboxylation of the acyloxyl radical gave β-mesylate radical **2**, which reacts reversibly by heterolytic fragmentation of the mesylate group to give a contact ion pair.[27] The contact ion pair lifetimes are in the picosecond time domain,[27] and these species solvate to solvent-separated ion pairs and then to free ions faster than the response times in our LFP studies. Thus, the processes evaluated by LFP are mainly those for the free radical cations. Moreover, the PhSH trapping results in the previous section demonstrated that equilibration between acyclic and cyclic distonic radical cations was established faster than processes studied by LFP methods. As noted earlier, the reactions are triggered by laser photolysis, but they are *not* photochemical reactions, which would be much faster than one can observe with the nanosecond-response photomultiplier tubes we used.

The first observed UV spectra in LFP studies displayed a broad, weak absorbance at 490 nm from the pyridine-2-thiyl radical.[37] Destruction of the PTOC ester precursor should result in bleaching in the region of 300−400 nm, and this was observed for reactions in CH_2Cl_2. For other solvents, the bleaching in the 300−400 nm range was small, suggesting the "instantaneous" formation of a transient with weak absorbance in this region.

(37) Alam, M. M.; Watanabe, A.; Ito, O. *J. Org. Chem.* **1995**, *60*, 3440−3444.

SCHEME 7

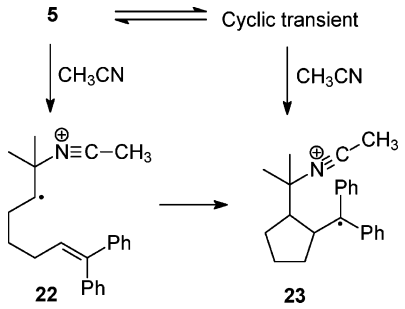

Among the possible products formed "instantly" in the LFP studies, 1,1-diarylethene radical cations have absorbances with $\lambda_{max} \approx 400$ nm,[38] diphenylalkyl radicals have $\lambda_{max} \approx 335$ nm,[35,36,39,40] and diphenylalkyl cations have $\lambda_{max} \approx 450$ nm.[26,38,41] We observed no strong signals in the region 300−450 nm in any of the initial spectra in TFT, CH_2Cl_2, and CH_3CN solvents, but strong signals from diphenylalkyl radicals grew in with time as discussed below. The absence of strong absorbances in the initial spectra was somewhat surprising, but an independent oxidation of diene **10** confirmed that the initially formed radical cations do not absorb strongly. Specifically, we oxidized diene **10** in a photoinduced electron transfer (PET) reaction using a chloranil triplet as the oxidant. Excitation of chloranil with 355 nm laser light gives the relatively long-lived triplet species, which is a strong oxidant that reacts with alkenes in diffusion-controlled processes.[26] When the chloranil triplet was produced by LFP in CH_3CN solvent in the presence of diene **10**, signals for the chloranil triplet decayed as this species oxidized **10**. New signals from diphenylalkyl radicals, with λ_{max} at ca. 330 nm, grew in with time, but no strong signals for the radical cation from **10** were observed in the first formed spectrum.[42]

The thiophenol trapping results require that the radical cations be equilibrated with subnanosecond half-lives. On the slower kinetic scale evaluated in the LFP studies, strong signals with $\lambda_{max} \approx 335$ nm grew in with time. Figure 3 shows typical results. The growing absorbances resembled those for diphenylalkyl radicals,[35,36,39,40] and the subsequent slow decay of these transients also resembled the behavior of diphenylalkyl radicals.[35,36,40] From these spectroscopic results and the product studies discussed above, reactions shown in Scheme 6 are important. The acyclic species is in rapid equilibrium with a cyclic transient that reacts relatively slowly as an acid, as an electrophile, or in a rearrangement reaction to give diphenylalkyl radical species such as **20**, **21**, and **8** that are observed spectroscopically.

Rate constants for the processes followed in the LFP studies are listed in Table 2. These reactions were orders of magnitude slower than those evaluated in the thiophenol trapping studies. The observed first-order or pseudo-first-order rate constants for

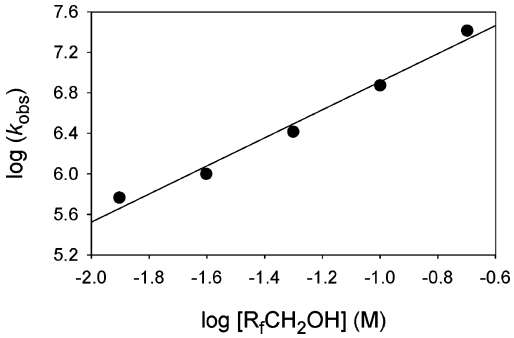

FIGURE 4. Rate constants from LFP studies at 20 °C as a function of the concentration of fluoro alcohol added to TFT solutions.

growth of the signal at 335 nm ranged from 2×10^5 s^{-1} to 6×10^6 s^{-1} at ambient temperature for trifluorotoluene (TFT), methylene chloride, and acetonitrile.

Table 1 lists values for k_{cycle} thus calculated for all solvents evaluated except benzene, in which the data were too scattered to give meaningful results. The errors in the values of k_{cycle} are at 2σ and reflect the precision of the experimental data.

The rate constants observed for CH_3CN solutions are similar to the rate constants found for reactions of a simple alkene radical cation in that solvent.[26] In those studies, the predominant process was reaction of CH_3CN as a nucleophile with the radical cation, a reaction that was previously observed by Arnold when alkene radical cations were produced in CH_3CN in photo-NOCAS reactions.[43] For the system studied here, however, acetonitrile capture of both the acyclic radical cation and the cyclic, distonic radical cation is possible, and the latter reaction should be fast. Thus, two predominant pathways for reactions are possible in this solvent, as illustrated in Scheme 7, and these cannot be differentiated from the LFP kinetic data. 5-*Exo* cyclizations of 6,6-diphenyl-5-pentenyl radicals have rate constants greater than 1×10^7 s^{-1} at ambient temperature,[35,36] and the cyclization of radical **22** in Scheme 7 is not likely to be rate limiting.

When fluorinated alcohols were added to TFT to increase the solvent polarity, the rate constants for signal growth increased considerably. A relatively linear plot of log k_{obs} vs the logarithm of the concentration of fluoro alcohol suggested that the alcohols reacted as bases and/or nucleophiles (Figure 4). The slope of the log/log plot is 1.4, suggesting that partially aggregated alcohol (average aggregation number of 1.4) was involved in rate-limiting processes. We note that the rate constants appeared to increase with solvent polarity (cf. reactions in TFT and in CH_2Cl_2), and it is possible that the kinetic effect of the fluoro alcohols was due at least in part to increasing solvent polarity with increasing concentrations of alcohol.

Variable-temperature kinetic results conducted over the temperature range −30 to 50 °C were quite unusual (Table 2 and Figure 5). The reaction in TFT appeared to be typical with a log A value of 10.1 and an activation energy of 6.3 kcal/mol. As the solvent polarity was increased by addition of increasing amounts of fluorinated alcohols, however, both log A and E_a values decreased dramatically and eventually reached values that are not possible for a simple reaction (Table 2).

The impossibly small log A terms and small or negative activation energies require that at least one fast equilibrium

(38) Ramamurthy, V.; Lakshminarasimhan, P.; Grey, C. P.; Johnston, L. J. *Chem. Commun.* **1998**, 2411−2424.

(39) Chatgilialoglu, C. In *Handbook of Organic Photochemistry*; Scaiano, J. C., Ed.; CRC Press: Boca Raton, FL, 1989; Vol. 2, pp 3−11.

(40) Newcomb, M.; Tanaka, N.; Bouvier, A.; Tronche, C.; Horner, J. H.; Musa, O. M.; Martinez, F. N. *J. Am. Chem. Soc.* **1996**, *118*, 8505−8506.

(41) Faria, J. L.; Steenken, S. *J. Phys. Chem.* **1993**, *97*, 1924−1930.

(42) An expectation that 1,1-diaryl alkene radical cations will absorb strongly at ca. 400 nm might be based on limited data. For example, PET oxidation of 1,1-diphenylethene and 1,1-diphenylbut-1-ene by the chloranil triplet in CH_3CN solution gave results similar to those with diene **10**. Weak signals centered at ca. 400 nm were observed.

(43) deLijser, H. J. P.; Arnold, D. R. *J. Org. Chem.* **1997**, *62*, 8432−8438.

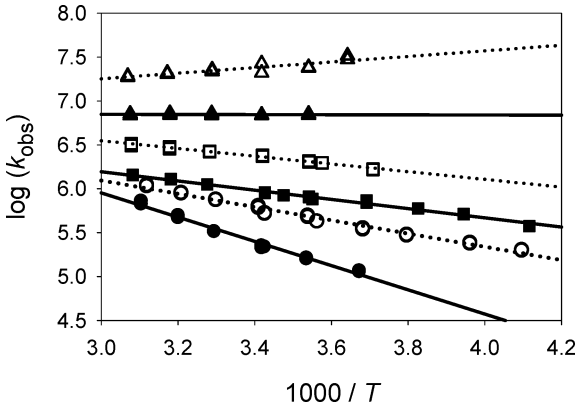

FIGURE 5. Arrhenius functions from LFP studies of **1** in TFT-containing fluoro alcohols. ●, TFT; ○, TFT/0.0125 M *n*-$C_7F_{15}CH_2$-OH; ■, TFT/0.025 M *n*-$C_7F_{15}CH_2OH$; □, TFT/0.05 M *n*-$C_4HF_8CH_2OH$; ▲, TFT/0.10 M *n*-$C_4HF_8CH_2OH$; △, TFT/0.20 M *n*-$C_4HF_8CH_2OH$.

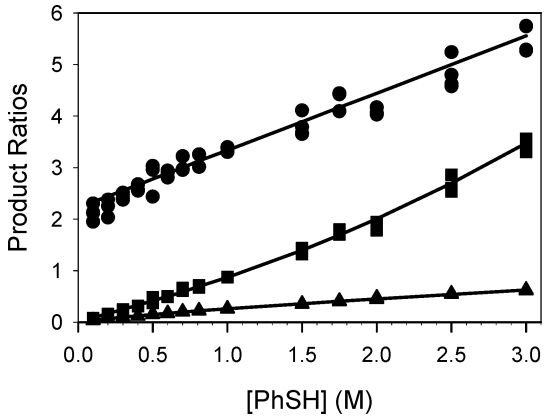

FIGURE 6. Product ratios from reactions in CH_2Cl_2. The symbols are experimentally determined ratios, and the lines are results from kinetic simulations. The plots are for the ratio [acycle **10**]/[cycle **11**] (●), the ratio [mesylate **9**]/[cycle **11**] (■), and the ratio [mesylate **9**]/[acycle **10**] (▲).

SCHEME 8

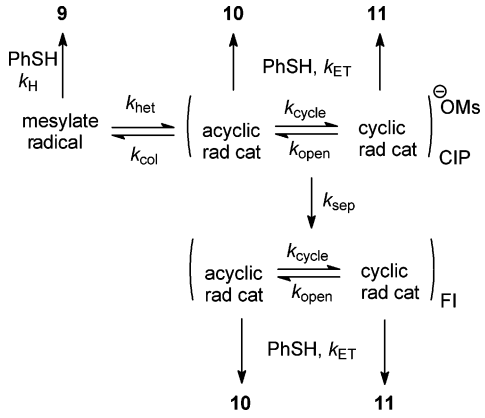

reaction precedes the rate-determining step. In such a situation, the observed log *A* value is the total of the log *A* of the initial reaction minus the log *A* of the back-reaction plus the log *A* of the second reaction. Thus, again, the LFP results are consistent with the dynamic situation suggested from the PhSH trapping results where rapid equilibration of acyclic and cyclic radical cations occurred. The distonic radical cation should be more strongly solvated due to its localized charge, and as the concentration of alcohol in the solvent is increased, the distonic radical cation might have a more extensively organized solvent shell, resulting in a ring-opening reaction with an increasing log *A* value with increasing alcohol concentration. Because the log *A* term for the back-reaction in the equilibration is a negative value in the total log *A* expression, increasing the entropy of the ring-opening reaction would reduce the overall entropy term for the reactions monitored in the LFP studies.

Kinetic Modeling. One method for evaluating the kinetic results for the radical cation reactions studied here and the mesylate heterolysis reactions previously reported[27] is to obtain rate constants by kinetic modeling and compare those empirical rate constants to the rate constants found with least-squares fits of analytical rate expressions such as eq 1. We performed kinetic modeling by numerical integration of the differential rate equations for the reaction sequence shown in Scheme 8,[44] which reflects the complexity of radical heterolysis reactions. In the presence of thiophenol, the β-mesylate radical **2** can be trapped in an H-atom transfer reaction by PhSH to give mesylate product **9**. The radical heterolysis reaction in competition with radical trapping is a multistep process. Reversible fragmentation of the mesylate radical gives a contact ion pair (CIP) containing acyclic radical cations in equilibrium with cyclic radical cations. Both radical cations can be trapped by PhSH in the ion pair, or they can escape to give free ions (FI). Thiophenol trapping of the acyclic radical cation gives diene **10**, and trapping of the cyclic radical cation gives mainly product **11**. The equilibrium constant for cyclization and ring opening of the radical cations is assumed to be the same in the CIPs and free ions.

Figure 6 shows results from kinetic modeling for reactions in CH_2Cl_2, which are typical. The symbols show experimental product ratios as a function of thiophenol concentration, and the lines show the predictions of those ratios from kinetic modeling. Note that there is no analytical expression for the ratio of mesylate **9** to cyclic product **11**, but the simulated behavior from the kinetic modeling is in excellent agreement with the observed ratio of products at various PhSH concentrations. In this example, the rate constants from modeling were $k_{het} = 6.5 \times 10^8$, $k_{coll} = 1.3 \times 10^{10}$, $k_{sep} = 1.7 \times 10^{10}$, $k_{cycle} = 1.8 \times 10^{10}$, and $k_{open} = 4 \times 10^{10}$ s^{-1}, where k_H for PhSH trapping of radical **2** was taken as 1×10^8 M^{-1} s^{-1} [45,46] and k_{ET} for PhSH trapping of any radical cation was assumed to be 2×10^{10} M^{-1} s^{-1}. All of the rate constants obtained empirically in kinetic modeling in this example and for other solvents were within 1 standard deviation of the least-squares values for the rate constants for radical heterolysis reactions[27] and the rate constants for cyclization and ring opening found in this work.

The modeling results not only lend support for the accuracies of the rate constants determined by least-squares solutions of the analytical rate expressions but also provide some insights about the limits on rate constants. For example, the model cannot be fit successfully under any circumstances when the radical cation cyclization and ring-opening reactions are not fast enough to establish an equilibrium between acyclic and cyclic radical cations in competition with PhSH trapping. We note, however,

(44) *PSI-Plot*, version 7.01 for Windows; Poly Software International Inc.: Pearl River, NY, 2002.

(45) Franz, J. A.; Bushaw, B. A.; Alnajjar, M. S. *J. Am. Chem. Soc.* **1989**, *111*, 268−275.

(46) Newcomb, M.; Choi, S. Y.; Horner, J. H. *J. Org. Chem.* **1999**, *64*, 1225−1231.

that any error in the assumptions that thiophenol reacts with both types of radical cations with diffusion-controlled rate constants would result in an error in the absolute values for rate constants obtained by modeling as well as those obtained by least-squares fits of the analytical expressions.

Conclusion

Both thiophenol trapping studies and laser flash photolysis kinetic studies indicate that the acyclic alkene radical cation formed from solvolysis of the mesylate group in radical **2** rapidly equilibrates with one or more cyclic radical cations. Computational results suggest that delocalized acyclic radical cation **5** is the lowest-energy species in the system studied here, and the kinetic studies are consistent with this conclusion. The 5-*exo* cyclization equilibrium is established faster than diffusion-controlled second-order reactions, and therefore, the product mixtures formed from this reaction manifold will be determined largely by the relative rate constants of competing follow-up reactions. Of considerable interest from the synthetic perspective, the removal of the phenyl groups in the various radical cation transients should have a relatively constant effect on all transients, leading to the conclusion that 5-*exo* cyclization of a simple 1,6-diene radical cation also should be fast with an equilibrium constant close to unity.

Experimental Section

The preparation of PTOC ester **1** and authentic samples of products from the radical reactions are described in the Supporting Information.

Reactions of 1 and Analysis for 9−13. Reactions of PTOC ester **1** were conducted in 8 mm (i.d.) Pyrex reaction tubes that were capped with rubber septa. The tubes were purged for at least 5 min with a continuous flow of N_2, and solvent (TFT, DCM, benzene, or ACN), thiophenol, and, in some cases, TFE were added to the reaction tube to give a total volume of 700 μL. The solutions were deoxygenated for 2−4 min by agitating them while passing through a gentle stream of N_2 from a syringe needle. The solutions were then shielded from light. The PTOC ester solution (300 μL, 0.033 M) was added, and the solution was further deoxygenated for 2−3 min as described above. The syringe needle was withdrawn, and the solution was irradiated with a 150 W tungsten floodlamp at a distance of ca. 0.5 m for 1−1.5 h. The reaction mixtures were analyzed directly by HPLC. Mixtures of methanol, acetonitrile, and water were used as eluant (typically 70:20:10, respectively) for 10 min, followed by a gradient (1 min) to a 70:30 mixture of methanol/acetonitrile, followed by further elution to 30 min.

Laser Flash Photolysis studies were performed with an Applied Photophysics LKS-50 laser kinetic spectrometer. The third harmonic (355 nm, 7 ns duration, 40−60 mJ/pulse) from a Continuum Surelite 1 laser was used in all LFP studies. Data from the photomultiplier were digitized using an Agilent infinium oscilloscope (model 54845a). When possible, oversampling (64/1) was used to improve S/N. Samples of radical precursor **1** were prepared in the appropriate solvent, and the concentration of **1** was adjusted to give an absorbance of 0.2−0.5 at 355 nm. The samples (typically 250 mL) were placed in a jacketed addition funnel and deoxygenated by a slow flow of helium. The temperature of the solution was adjusted by circulating a temperature-regulated methanol/water mixture through the external jacket with a circulating bath. The sample was equilibrated at the desired temperature for 10−20 min and then allowed to flow through a flow cell at a rate of 5−20 mL per min. The sample temperatures were measured by a thermocouple inserted into the flow cell just above the laser and analyzing light paths. For low-temperature data, the sample and cuvette were enclosed in a box equipped with quartz windows that was purged with nitrogen to minimize water condensation on optical surfaces.

Acknowledgment. This work was supported by a grant from the National Science Foundation.

Supporting Information Available: Synthetic details, tables of product yields, tables of computational results, and NMR spectra. This material is available free of charge via the Internet at http://pubs.acs.org.

JO061868W